

Microstructural and Aqueous Corrosion Aspects of Laser-Surface-Melted Type 304 SS Plasma-Coated Mild Steel

M.G. Pujar, R.K. Dayal, and R.K. Singh Raman

Plasma spray deposition of metals, ceramics, or plastics onto base metals to produce wear- and corrosion-resistant surfaces is a promising technique whereby base metal performance can be considerably improved. Because these coatings invariably contain pores, voids, and cracks, laser surface melting may be employed to improve their homogeneity. This study focuses on the corrosion performance of laser-surface-melted type 304 SS plasma-coated mild steel specimens. Mild steel strips were plasma coated with an approximately 100 to 200 μm thick layer of type 304 by transferred plasma jet. These specimens were subsequently laser irradiated using a 3 kW continuous-wave CO_2 gas laser. Eight different sets of specimens were selected based on different laser beam travel speeds. Scanning electron microscopic studies of the plasma-coated specimens revealed both pancake and flowery types of deposited particles. Optical microscopic studies followed by anodic polarization experiments were carried out on these specimens in 1N H_2SO_4 medium. It was observed that specimens with laser beam interaction times ranging from 30 to 120 ms showed relatively better general corrosion performance than specimens with interaction times of from 15 to 24 ms.

Keywords

plasma coating, laser surface melting, aqueous corrosion

1. Introduction

ION implantation, plasma spraying, and laser surface melting (LSM) are among the surface modification techniques widely used in various industrial applications as well as in research laboratories. In general, the surface modification obtained by these techniques can be used to enhance wear and corrosion resistance. Study of their merits and drawbacks enables judicious selection of the proper surface modification method for a particular application.

Deposition of an overlay coating is a conventional technique for improving the corrosion and oxidation behavior of a less noble substrate (Ref 1). Plasma spraying represents one such method; because of its flexibility, it can be used to spray any material onto any type of substrate. Applications of plasma spraying include formation of corrosion-, temperature-, and abrasion-resistant coatings and production of monolithic shapes that take advantage of the rapid solidification process. However, one limitation of such coatings is surface-connected porosity (Ref 2, 3). Other limiting factors are the rough coating surface and the weak physical bonding between the substrate and the coating (Ref 4). These plasma coatings could be further improved to avoid decohesion either by high-temperature heat treatment or by LSM, which not only increases the density of the coating by sealing the pores but also improves its microstructure through rapid solidification (Ref 5).

M.G. Pujar, R.K. Dayal, and R.K. Singh Raman, Metallurgy Division, Indira Gandhi Centre for Atomic Research, Kalpakkam 603 102, India

Laser surface alloying has been hailed as a new technique whereby desired alloy composition can be achieved in-situ on a workpiece surface with the help of laser beam heating. The addition of alloying elements in the form of powder or a thin coating during laser beam heating results in the localized melting of the substrate to form an entirely different surface, with a different composition and microstructure. Many recent applications exemplify the importance of laser surface melting and alloying to improve substrate properties (Ref 6-15).

Although plasma spraying and LSM are two distinct processes, they have a common utility: to modify the substrate surface and make it more resistant to corrosive environments. Mild steel is extensively used in power-generating industries. Because this material is highly prone to aqueous corrosion in acidic medium, modification of its surface is of prime importance, especially for large components where use of a corrosion-resistant alloy such as stainless steel as the primary construction material would not be cost effective.

This study focuses on the aqueous corrosion resistance of type 304 SS plasma-coated mild steel in a sulfuric acid medium. An anodic polarization technique was used to study general corrosion behavior. The specimens were inspected using optical and scanning electron microscopy (SEM), and electron probe microanalyzer (EPMA) line scanning data (Ref 16) were used to explain the results.

2. Experimental Methods

2.1 Specimens

The specimens had been earlier prepared for high-temperature oxidation studies (Ref 16); unused specimens were utilized for this investigation. They were of mild steel (100 by 50 by 3 mm) and were coated with an approximately 100 to 200 μm thick layer of type 304 stainless steel powder deposited by the plasma torch method. The nominal chemical composition (in

Table 1 Laser travel speeds and LSM zone thickness values for type 304 SS plasma-coated mild steel

Specimen designation	Laser beam travel speed, mm/min	Interaction time, ms	LSM zone thickness, μm
LT1	2000	15	Negligible
LT2	1750	17	Negligible
LT3	1500	20	Negligible
LT4	1250	24	Negligible
LT5	1000	30	100-200
LT6	750	40	100-200
LT7	500	60	100-200
LT8	250	120	100-200

weight percent) of the mild steel specimens was 0.18% C, 0.4% Mn, 0.06% S, and 0.06% P; that of the plasma feed was 18% Cr and 8% Ni. The specimens were then laser irradiated in an argon shielding environment using a 3 kW continuous-wave (CW) CO₂ gas laser. The interaction time for different specimens was varied by changing the laser beam travel speed from 250 to 2000 mm/min to achieve an interaction time range of 120 to 15 ms for a 0.5 mm laser beam diameter (Table 1). Eight different sets of specimens were obtained by using laser beam travel speeds of 2000, 1750, 1500, 1250, 1000, 750, 500, and 250 mm/min. The specimens pertaining to these travel speeds were designated as LT1, LT2, LT3, LT4, LT5, LT6, LT7, and LT8, respectively.

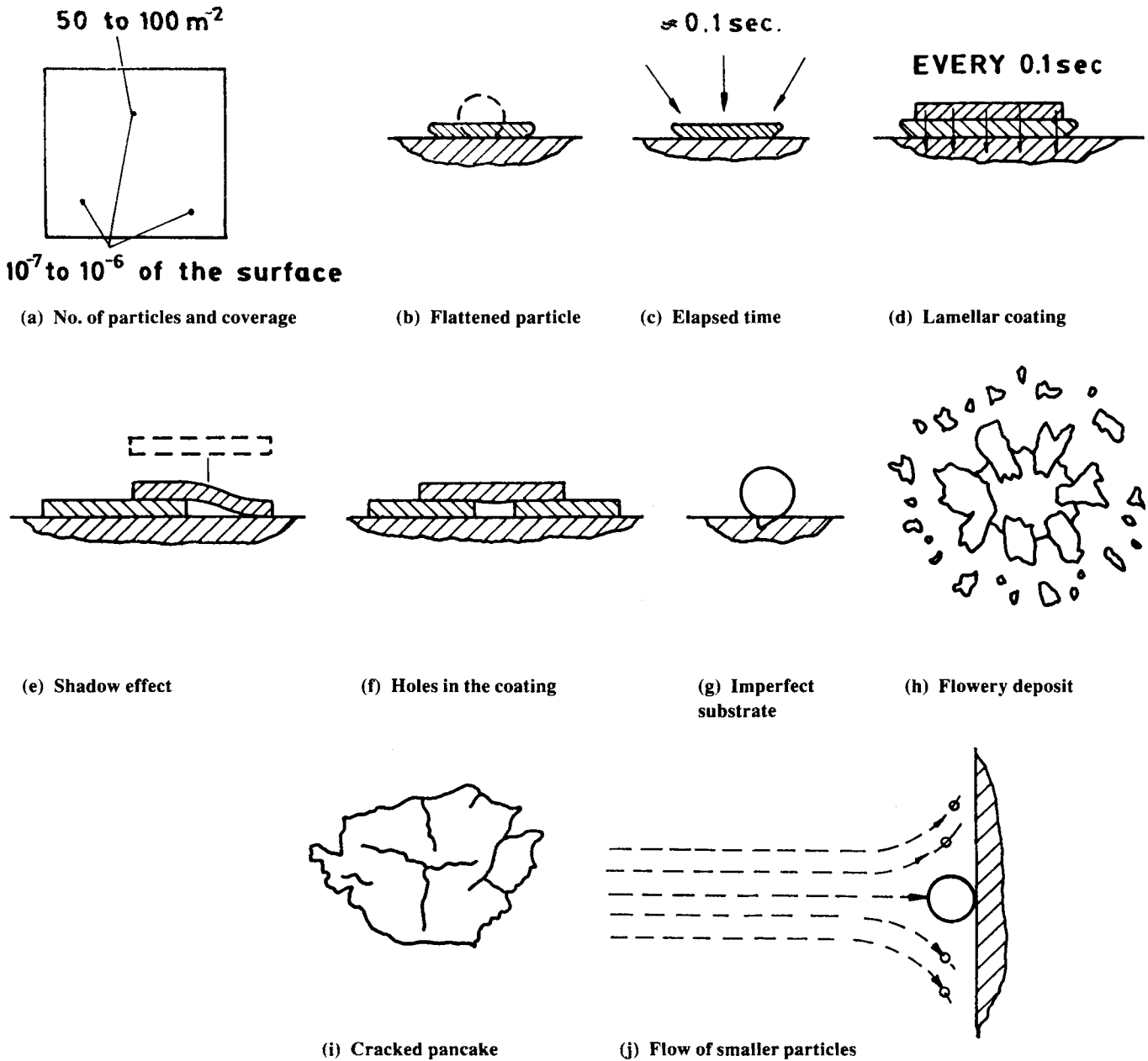


Fig. 1 Different processes that take place during plasma spraying. Source: Ref 18

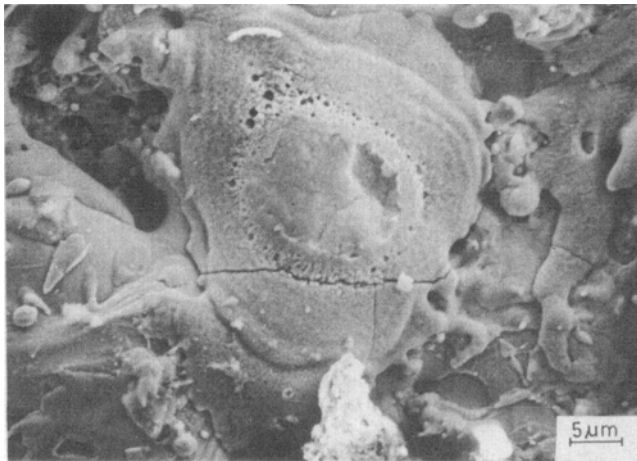


Fig. 2 SEM micrograph showing a pancake-type deposit obtained during plasma coating of mild steel

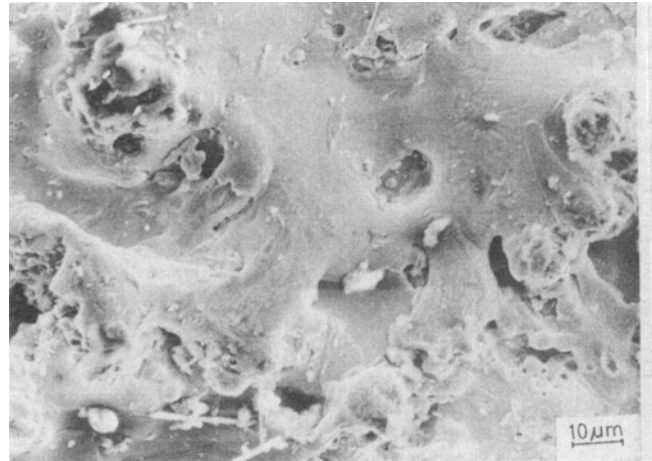


Fig. 3 SEM micrograph showing inhomogeneous, porous deposit of type 304 SS powder plasma sprayed onto mild steel

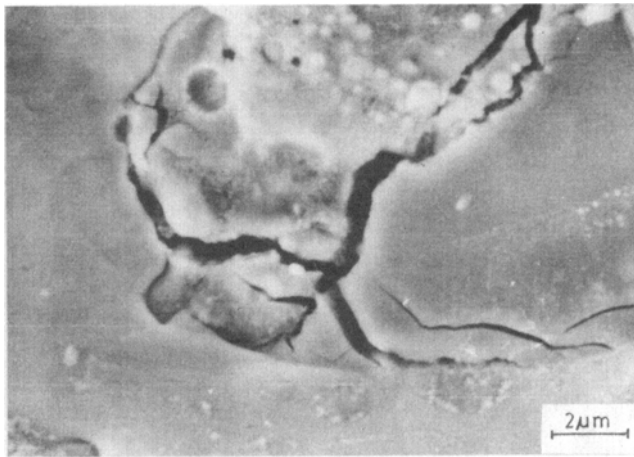


Fig. 4 SEM micrograph showing a severely cracked pancake-type deposit

2.2 Optical Microscopic and EPMA Line Scanning Studies

The plasma-coated mild steel specimens were cut and mounted in epoxy resin to expose the cross sections and then polished to a fine diamond (1 μm) finish, chemically etched with nital, and observed under the optical microscope. The thicknesses of the LSM zone for each specimen are given in Table 1. Concentration profiles were obtained earlier (Ref 16) for chromium, nickel, and iron across the plasma coating and LSM zones using the EPMA line scanning technique.

2.3 Aqueous Corrosion Studies in Sulfuric Acid Medium

The laser-melted and cut specimens were mounted in epoxy resin for electrochemical studies, with the coated surface exposed to the electrolyte. Anodic polarization experiments were carried out in 1N H₂SO₄ solution, which was continuously deaerated by bubbling oxygen-free pure hydrogen gas through

it. All electrode potential measurements were carried out with respect to a saturated calomel electrode (SCE), and the potential scan rate was maintained at 10 mV/min. The anodic polarization experiments were started from a cathodic potential of -600 mV (SCE) and were continued until attainment of transpassivity. In the case of LSM type 304 plasma-coated specimens, only a single anodic polarization experiment could be carried out on each specimen because of extremely high active dissolution and high passive currents. For comparison, anodic polarization curves were also obtained for non-LSM type 304 plasma-coated specimens.

3. Results and Discussion

3.1 Characterization of the Coatings and LSM Zone

The deposits obtained by transferring a plasma jet onto a charged substrate (anode) are essentially nonuniform (Ref 17). The various processes that take place during the generation of plasma-sprayed coatings are excellently described by Zaat (Ref 18). This model, shown in Fig. 1, describes the formation of cracks and voids during the plasma spraying process. The particles exit the nozzle of the plasma torch with a high kinetic energy, impinge on the target (substrate), and become flattened—thereby giving rise to what is known as pancake type of deposit (Fig. 2). This type of coating is built particle by particle, creating a lamellar structure. Also, because of a shadow effect (Fig. 1) that occurs during the coating process and the existence of narrow holes (Fig. 1) on the imperfect substrate surface, the coatings are invariably inhomogeneous in nature (Fig. 3). As shown in Fig. 4, the deposits can become severely cracked due to tension stresses that arise during expansion of the substrate and simultaneous cooling of the pancake (Ref 19).

Figure 5 shows a perfect “flowery” type of deposit in the plasma-sprayed coating that has settled over an already existing pancake-type deposit. The contact between the pancake-type deposit and the substrate is much better than that between the flowery deposit and the substrate due to better wetting of the substrate surface in the former case (Ref 19). It has been

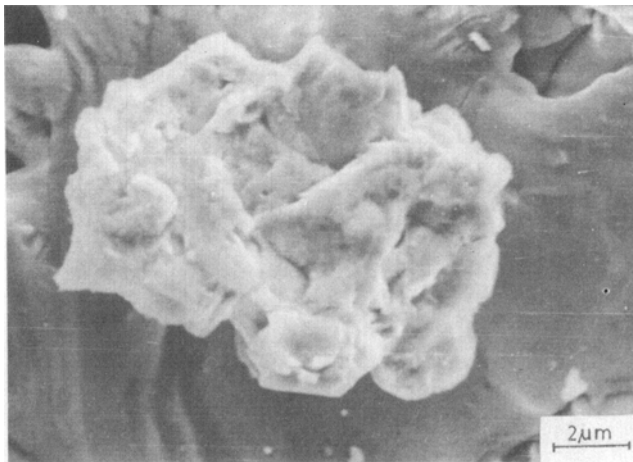


Fig. 5 SEM micrograph showing a “flowery” type of deposit over a pancake-type deposit

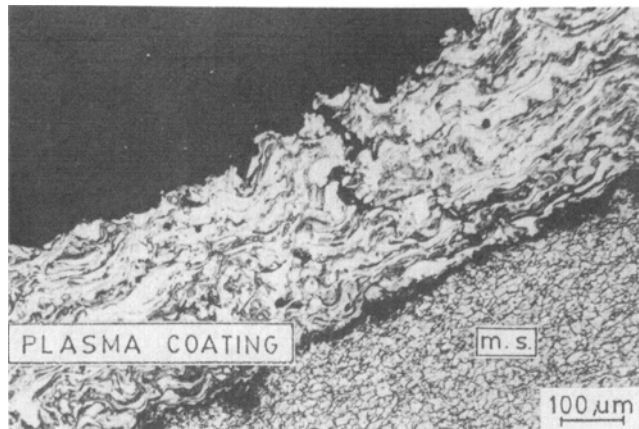


Fig. 6 SEM micrograph of the type 304 SS plasma deposit showing columnar grain growth in the pancakes

found that wetting and flow properties of the liquid droplets of the coating material are of primary importance, because they influence the porosity and the mechanical anchorage between the successive layers of the deposit (Ref 20).

This is also reflected in the corrosion behavior of the specimens. As the deposit thickness increases due to addition of successive lamellae, thermal conduction to the substrate gradually decreases; the coating surface temperature increases until an equilibrium is attained whereby heat is primarily lost from the newly formed coated surface to the environment. At this stage, solidification of the individual particles is slowed, and remelting of the surface (previously solidified lamellae) and fusing with the lamella above it take place. This phenomenon is known as microwelding. During the solidification of such microwelded lamellae, columnar grain growth occurs perpendicular to the substrate surface (Ref 21, 22). An SEM micrograph (Fig. 6) taken from the top surface of the plasma coating shows such a columnar grain growth.

As described above, coatings applied by the transferred plasma jet process have inherent structural inhomogeneities across their thickness. Laser surface melting treatment ho-

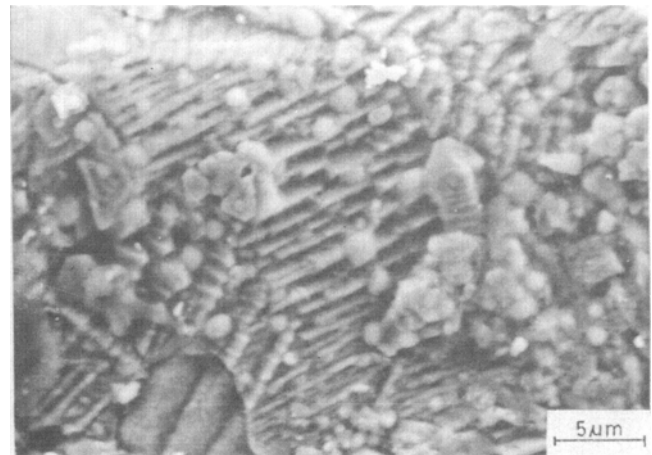


Fig. 7 Optical micrograph (cross section) of the type 304 SS plasma coating on mild steel showing a lamellar structure with cracks. Etched in 2% nital

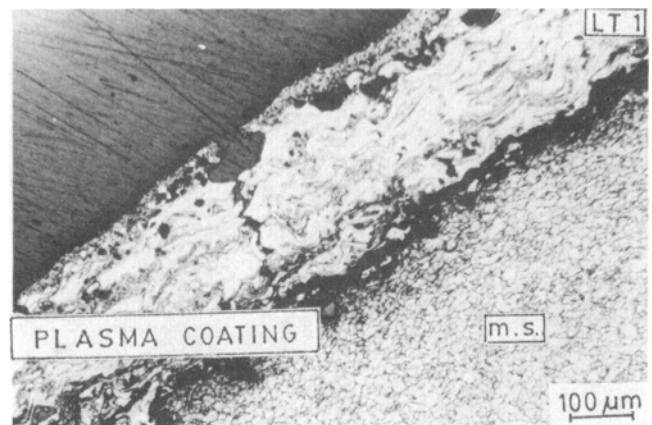


Fig. 8 Optical micrograph (crosssection) of an LSM-treated specimen (LT1) showing imperfect laser sealing and cracks in the coating. Etched in 2% nital

mogenizes the coatings and eliminates the inherent defects by means of rapid surface melting and cooling to form a flawless LSM zone. An optical micrograph depicting the cross section of the lamellar, porous, and cracked plasma-sprayed coating is shown in Fig. 7. It is clear from Table 1 that as the laser processing speeds vary from 2000 to 1250 mm/s, the interaction time changes from 15 to 24 ms (specimens LT1 to LT4). Due to this lower interaction time, an insignificant and nonuniform melted zone is formed, which does not seal the underlying cracks and pores in the deposit (Fig. 8). In the second group of specimens (LT5 to LT8), the interaction time was increased significantly, resulting in complete melting of the coating and formation of a uniform, pore-free, coherent LSM zone (Fig. 9).

3.2 Aqueous Corrosion Resistance in Sulfuric Acid Medium

Anodic polarization curves obtained for specimens LT1 to LT4 and for specimens LT5 to LT8 are shown in Fig. 10 and 11, respectively, along with curves for the non-LSM type 304

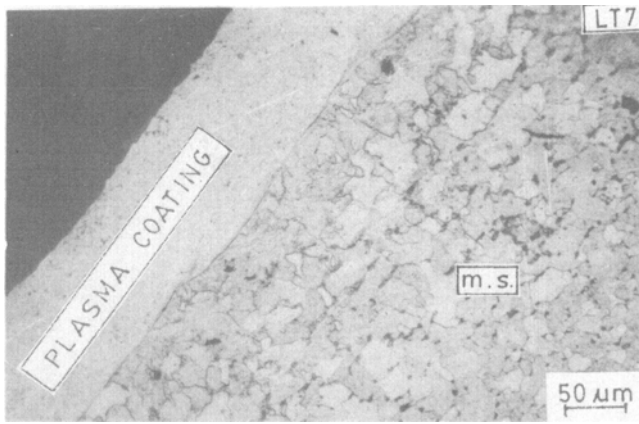


Fig. 9 Optical micrograph (cross section) of an LSM-treated specimen (LT7) showing a homogeneous, defect-free LSM zone. Etched in 2% nital

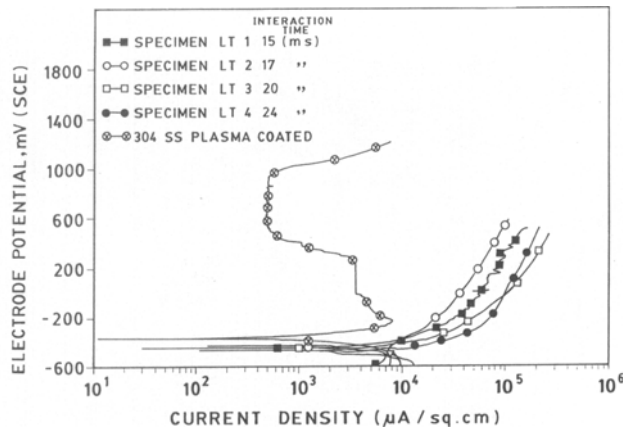


Fig. 10 Anodic polarization curves for type 304 SS plasma-coated and type 304 SS plasma-coated + laser-treated mild steel specimens in 1N H₂SO₄ medium

plasma-coated specimen. It is clear from Fig. 10 that specimens LT1 to LT4 continuously dissolved in the 1N H₂SO₄ medium without ever attaining passivity. The current-density values obtained during anodic dissolution were extremely high. During experimentation it was observed that the plasma-coated layer slowly crumbled into the solution, exposing the mild steel surface beneath it and further accelerating dissolution. This phenomenon, wherein failure of the plasma coating takes place at the interface of the coating and the substrate surface during service is known as adhesive failure (Ref 23). It indicated an imperfect laser sealing treatment of the specimen due to very high laser beam travel speed, which resulted in insufficient interaction time.

In contrast, Fig. 11 shows that specimens LT5 to LT8 exhibited perfect active-passive curves and transpassive dissolution. All of these anodic polarization curves were nearly identical, with very high active peak current density, very high passive current density, and much higher transpassive potential values as compared to the non-LSM type 304 plasma-coated specimen. An important feature noted during the anodic polarization

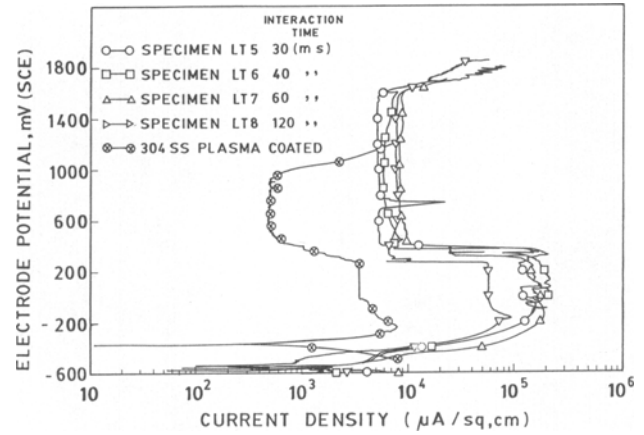


Fig. 11 Anodic polarization curves for type 304 SS plasma-coated and type 304 SS plasma-coated + laser-treated mild steel specimens in 1N H₂SO₄ medium

was the spontaneous breakdown of the unstable passive film at several indistinct points from the corroding surfaces of these specimens, giving rise to sudden active dissolution spanning a few tens of millivolts (SCE) (Fig. 11, specimen LT5). Therefore, it was concluded that the film that formed over the corroding surface was not a true passive film, but a loose corrosion-deposit film that was porous and enabled the metal ions beneath it to exit freely and dissolve in the solution. The higher current-density values exhibited by the plasma specimen could be correlated to the apparent specimen area and not to the true specimen area, which was much higher because of the numerous particles deposited on the surface. Taking this fact into account, it was concluded that the actual current-density values could be orders of magnitude lower than those shown in Fig. 10 and 11 for the plasma-coated specimen.

These conclusions are in perfect concurrence with the EPMA scan results shown in Fig. 12. The plasma-coated specimen contained 17 to 18% Cr and 8 to 9% Ni across an initial 100 to 200 μm thickness. The composition of this surface confirmed that the plasma-coated surface of mild steel consisted of type 304 stainless steel. This explains the better corrosion resistance exhibited by the plasma-coated mild steel specimen without laser treatment, although the active and passive current-density values are slightly higher owing to the porosity of the coating. Specimens LT5 to LT8 contained less than 4% Cr and less than 3% Ni. This suggested a complete melting of the plasma coating and dilution of its constituents due to alloying with the substrate during the laser surface treatment. The low levels of chromium and nickel in these specimens are reflected in the extensive active dissolution and formation of loose corrosion-deposit film during passivation.

In specimens LT1 to LT4, continuous dissolution and crumbling of the coating (adhesive failure) during the anodic polarization experiment was observed. The short interaction times may have caused the laser beam to induce some decohesive effect between the coating and the substrate. Sealing of the surface-connected porosity of such coatings is vital. This could be achieved by melting a small layer of the surface material and keeping it in the liquid phase until surface tension smoothed out

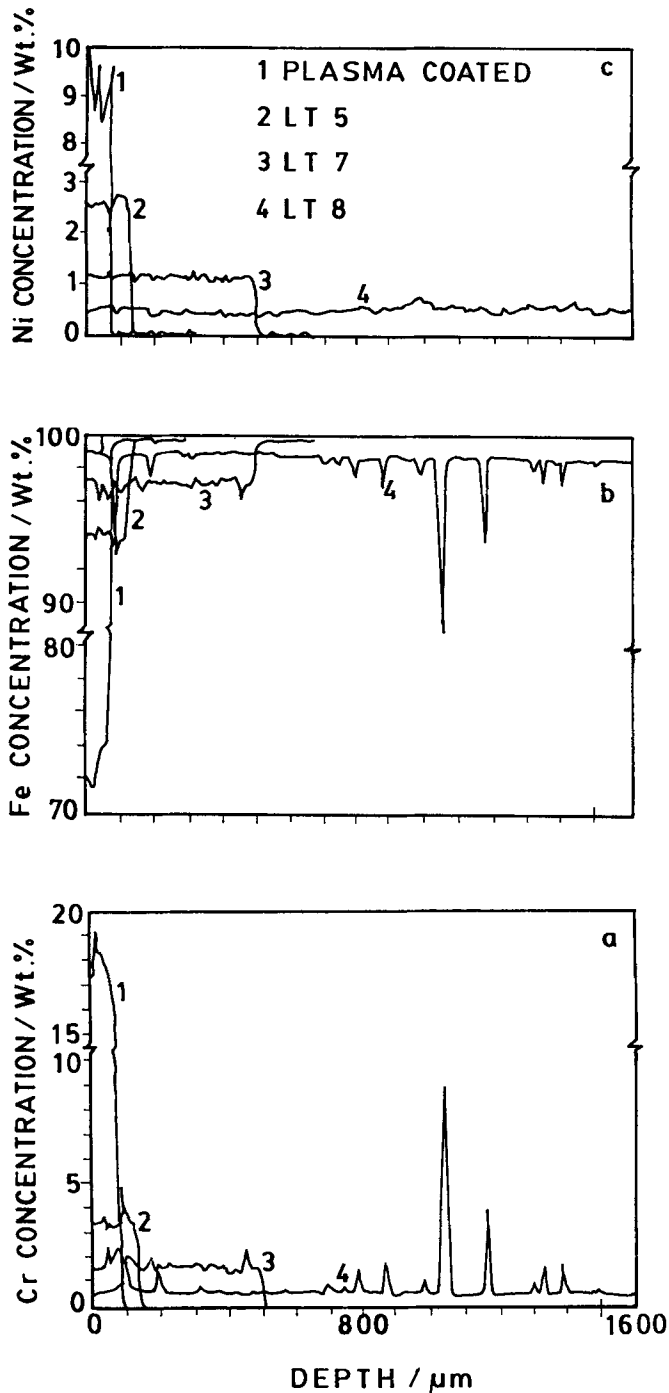


Fig. 12 Concentration profiles of (a) nickel, (b) iron, and (c) chromium by EPMA line scanning

any surface discontinuities; however, surface vaporization must be avoided (Ref 24).

According to Ref 3, when laser surface treatment is carried out on such plasma coatings to affect the top 25 μm layer, proper pore sealing and homogenization are achieved. In the particular investigation described here, the LSM zone thickness values were either negligibly low (specimens LT1 to LT4)

or greater than 100 to 200 μm (specimens LT5 to LT8) (Table 1). These results suggest that a different set of LSM treatment parameters would have produced specimens with better corrosion resistance than the non-LSM plasma-coated specimen. It is also important to incorporate an intermediate thin bond coat to avoid adhesive failure.

4. Conclusions

The aqueous corrosion resistance of eight mild steel specimens plasma coated with type 304 SS to 1N H₂SO₄ medium was studied after laser surface melting by a CW CO₂ laser. The following conclusions can be drawn regarding the comparative corrosion resistance of these specimens:

- Laser-surface-melted zone thickness values ranged from 100 to 200 μm.
- The type 304 plasma-coated deposits exhibited distinct pancake and flowery types of morphologies, indicating partial wetting of the substrate by the plasma-coated particles.
- Lower interaction times (15 to 24 ms) resulted in incomplete homogenization and negligible LSM zone formation, and the remaining defects caused high active dissolution and unattainment of passivity.
- Higher interaction times (30 to 120 ms) allowed complete homogenization and dilution of alloying elements in the coating, thereby increasing active and passive dissolution of the LSM zone.
- Specimens with interaction times of from 30 to 120 ms showed better corrosion performance compared to specimens with interaction times of from 15 to 24 ms.
- Corrosion resistance could be further improved by modifying a smaller thickness of the coated layer through selection of appropriate laser processing parameters.

Acknowledgments

The authors thank Shri J.B. Gnanamoorthy, Head of the Metallurgy Division of IGCAR, for his keen interest during the course of this study. They also thank Dr. A.S. Khanna, Indian Institute of Technology (Bombay), and Dr. Kruetz, Fraunhofer Institute for Lasertechnik (Aachen, Germany), for providing the plasma-coated and laser-treated specimens. Thanks are also due to Smt. M. Radhika for the SEM examination of the specimens.

References

1. R.F. Smart and J.A. Catherall, in *Plasma Spraying*, Mills & Boon, London, 1972
2. M.L. Capp and J.M. Rigsbee, *Mater. Sci. Eng.*, Vol 62, 1984, p 49
3. H. Bhat, H. Herman, and R.J. Coyle, in *Proceedings of the Symposium High Temperature Protective Coatings* (Atlanta), S.C. Singhal, Ed., TMS-AIME, 1983, p 37
4. J.M. Rigsbee, *J. Met.*, Vol 36, 1984, p 31
5. P.G. Moore, in *Proceedings of International Symposium on Fundamental Aspects of Corrosion Protection by Surface Modification*, E. McCafferty, C.R. Clayton, and J. Oudar, Ed., Electrochemical Society, 1984, p 102
6. C.W. Draper and J.M. Poate, *Int. Met. Rev.*, Vol 30, 1985, p 85

7. S. Chiba, T. Sato, A. Kawashima, K. Asami, and K. Hashimoto, *Corros. Sci.*, Vol 26, 1986, p 311
8. D.S. Gnanamothu, in *Applications of Lasers in Materials Processing*, E.A. Metzbower, Ed., American Society for Metals, 1979, p 177
9. W.M. Steen, in *Proceedings of Second European Conference on Laser Treatment of Materials* (Bad Nauheim), 1988, p 60-64
10. P.G. Moore and E. McCafferty, *J. Electrochem. Soc.*, Vol 128, 1981, p 1391
11. J. Mazumder and J. Singh, *High Temp. Mater. Process.*, Vol 7, 1986, p 101
12. E. McCafferty, G.K. Hubler, P.M. Hatishan, P.G. Moore, R.K. Kant, and B.D. Sartwell, *Mater. Sci. Eng.*, Vol 86, 1987, p 1
13. U. Kamachi Mudali, R.K. Dayal, J.B. Gnanamoorthy, S.M. Kanetakar, and S.B. Ogale, *Mater. Trans. JIM*, Vol 33, 1991, p 845
14. U. Kamachi Mudali and R.K. Dayal, *J. Mater. Eng. Perform.*, Vol 1, 1992, p 341
15. N. Parvathavarthini, R.K. Dayal, R. Sivakumar, U. Kamachi Mudali, and A. Bharathi, *Mater. Sci. Technol.*, Vol 8, 1992, p 1070
16. A.S. Khanna, R.K. Singh Raman, E.W. Kruetz, and A.L.E. Terrence, *Corros. Sci.*, Vol 33, 1992, p 949
17. L.G. Davis, *Can. Mach. Manuf. News*, Vol 70, 1959, p 49
18. J.H. Zaat, *Ann. Rev. Mater. Sci.*, Vol 13, 1983, p 9m to 42m
19. J.M. Houben, in *Proceedings of the 2nd American Thermal Spraying Conference* (Long Beach, CA), 31 Oct-2 Nov 1984, American Society for Metals, 1985, p 1
20. P. Fauchais, J.F. Coudert, A. and M. Vardelle, A. Grimaud, and P. Roumilhac, in *Proceedings of the National Thermal Spray Conference* (Orlando, FL), 14-17 Sept 1987, ASM International, 1988, p 11
21. G. Johner, V. Wilms, K.K. Schweitzer, and P. Adam, in *Proceedings of the National Thermal Spray Conference* (Orlando, FL), 14-17 Sept 1987, ASM International, 1988, p 155
22. G.N. Heintze and R. McPherson, in *Proceedings of the National Thermal Spray Conference* (Orlando, FL), 14-17 Sept 1987, ASM International, 1988, p 271
23. C.C. Berndt and R. McPherson, in *Adhesion of Plasma Sprayed Ceramic Coatings to Metals*, J. Pask and A. Evans, Ed., Plenum Press, 1981, p 619-628
24. S. Dallaire and P. Cielo, *Metall. Trans.*, Vol 13B, 1982, p 479